Synchronous Flyback Converter Coupled with Fuzzy Logic Control Efficiently Controls a Serially Connected VRLA Battery String

Charnyut Karnjanpiboon [1,*] and Kammon Jirasereeamornkul [2]

Abstract

This paper presents a high efficiency charge equalization system for balancing the energy in a serially connected, valve-regulated, lead acid battery string using a synchronous flyback converter. Each flyback converter was coupled through a DC-link bus in order to increase the overall energy transfer efficiency of the system and to eliminate the problem of unbalanced charging of the batteries. To ensure that the charge equalization system operated smoothly and safely charged the batteries, a fuzzy logic controller was used in the control section of the system. The validity of this approach was confirmed by computer simulation and by experimentation. The efficiency of this synchronous flyback converter was 78.9 percent, better by approximately 1.07 percent than the conventional flyback converter.

Keywords: Battery management system, Charge equalization system, Bi-direction flyback, Synchronous flyback, Fuzzy logic.

(Selected from 1st Symposium on Hands-on Research and Development, Chiang Mai)

[1] Department of Electrical Engineering Rajamangala University of Technology Lanna, Nan.

[2] Department of Electronic and Telecommunication Engineering, King Mongkut's University of Technology Thonburi, Bangkok

[*]Corresponding author, E-mail: chanyut@rmutl.ac.th Received 1 August 2011; Accepted 7 December 2011

1. Introduction

Valve-regulated, lead acid (VRLA [1-2]) is a secondary type battery that stores electrical energy as chemical energy. It is a serially connected battery string and an important DC power source for many modern electrical appliances. It is used in electric vehicles (EVs), Internet data centres (IDCs), telephone exchanges, banks, uninterruptible power supplies (UPSs), industries, and hospitals. The VRLA battery is an attractive component because it is economical and it has the capability to distribute a high surge current to a load. However, it has some drawbacks. VRLA batteries used in serially connected battery strings (SCBS) are not uniform in their chemical energy state, even though they were assembled in the same production line. In addition, the cycling of the charging and discharging processes cause the chemical energy of each battery in a SCBS to rapidly differ from that of the neighbouring battery, thus creating an imbalance. As a consequence some batteries overcharge, while others undercharge, and this effect shortens their service life.

To manage the imbalanced energy in a SCBS, a battery management system (BMS) is employed, and one important part of the BMS is the charge equalizing system (CES). This system transfers the excess energy from source battery to target battery. There are two techniques to operate a CES in a BMS: dissipative [3,4] and non-dissipative [5-16]. The non-dissipative technique was selected for this study because the efficiency of the former technique is extremely low. In the CES the equalizing circuit consists of an active switching circuit and this circuit performs the balancing operation. The operation can be catalogued into four main major approaches [5-7, 17]. The one that presents the greatest advantage is equalizing by allowing excess energy from a fully charged battery to flow through a DC-link bus and then sending this excess energy back to the targeted battery [16]. The differences between a DC-link bus topology and a traditional balancing topology (Fig. 1(a)) can be explained by the energy balancing process of passing the excess energy from battery number 4 to battery 1.

Using the traditional and the DC-link techniques of how to balance the excess energy were studied. The advantage of the DC-linked technique over other traditional techniques was clearly that the total efficiency of transferred energy did not depend on the total number of active converters. It only depended on the efficiency of the two active converters associated with the source and target batteries. Although a large distance may separate the source and target batteries, the total efficiency of transferred energy was still the same and its value close to one. (Note: To operate this technique at full capability, the number of SCBS must equal or be more than three units). In all traditional CES for SCBC, the efficiency of the transfer of the total energy is overlooked. There are two ways to increase the efficiency of the total energy transferred of the system. First, the system must use a high efficiency converter. Second, the system should use the proper energy transfer strategy. The proper strategy to transfer energy to the SCBS is to increase the efficiency of the flyback (FB) converter by synchronizing it using a DC-link bus.

This paper presents a synchronous flyback (SFB) converter topology that minimized the energy loss in the switching operation of a secondary switch in a standard bidirectional FB converter. The reduction of the energy loss was accomplished by replacing an active-switch, a MOSFET, for the diode typically used as the secondary switch of the FB converter. Because the turn-on resistance of the MOSFET is typically only $10x10^{-3}$ ohm, its losses for the same current were minimal compared to the diode with its higher forward voltage drop. A fuzzy logic control technique

was proposed [17], however it used a different low efficiency bi-directional CES topology.

In taking full advantage of the suitability of fuzzy logic controlling a nonlinear plant like a VRLA battery string, the design of the high efficiency charge equalization system was augmented with SFB converters and proven experimentally to be more efficient than the other approaches that were considered.

2. The balancing operation

Referencing Fig. 1(b), in the traditional method the excess energy from battery number 4 moves to battery 3 through converter number 3, then this energy moves to battery 2 by passing through converter 2 (Fig. 1(c)), at which point, the energy flows forward to battery 1 through converter 1 (Fig. 1(d)). For this process, the energy-transfer efficiency can be calculated using equation (1). We assumed that each converter had efficiency equal to 70 percent. By the calculation, the 100 percent excess energy from battery number 4 was reduced to 34.3 percent for battery 1.

Equation 1 is used to calculate the energy efficiency for the traditional case (case 1), while equation (2) gives the efficiency for the DC-linked method.

$$\eta_T = (\eta_c)^n \quad (1)$$

$$\eta_T = 2\eta_c \quad (2)$$

where

η_T is a total system transferred efficiency

η_c is the efficiency of each converter

n is the number of active converters

In the second case considered, the balancing process uses a DC-Link method (Fig. 1(e)). The excess energy from battery number 4 flows only to two converters; converters number 3 and 1 (Fig. 1(f)). The energy flows through a linked path between converter number 4 and converter 3, called the DC-Link bus. This DC-Link bus is the shortest way for energy to flow from one converter to another.

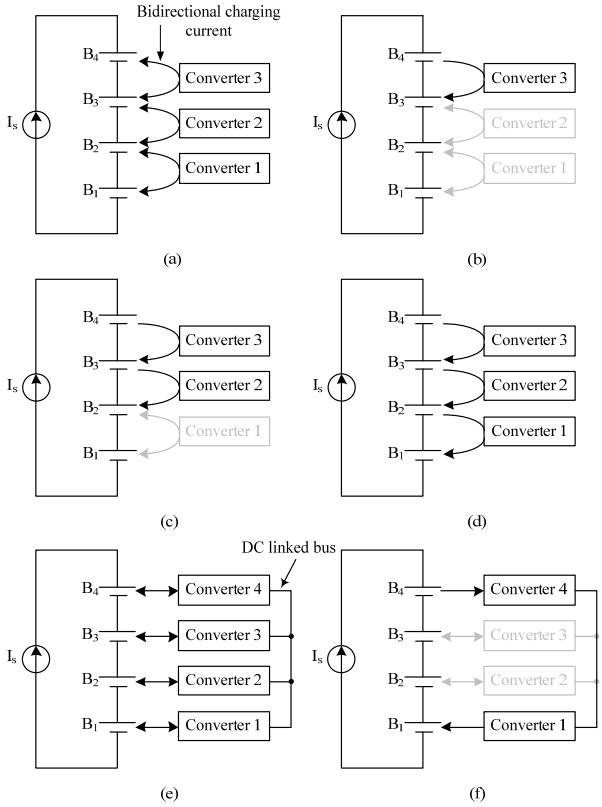

Fig. 1 Comparison of the balancing process of the traditional technique and the DC-Link technique

To compare the DC-Link method with the traditional method, the converter efficiency was selected to be equal to the traditional equalizing method (70 percent). The excess energy from battery number 4 transferred to battery 1 by an amount of 49 percent of the source energy, higher than the traditional case.

To better understand the traditional balancing process, a 3D efficiency transfer graph was constructed and analyzed, Karnjanapiboon (2009). This knowledge helped design the alternative.

The second approach, as proposed in [16], uses the positive relationship between converter efficiency and total efficiency to propose a double stage system for passing excess energy directly through a DC-link bus. When equalizing the excess energy is in process, only two converters are active, and therefore, the total energy transferred from source to target depends only on the efficiency of these two converters. In this technique, bidirectional switching FB converters are used in the charge equalization system. In general, the efficiency of the FB converter is 60 to 75 percent and the heat losses at a secondary switch are high. One choice to increase the efficiency of a FB converter is to reduce the conduction loss of the secondary switch by using a synchronous scheme.

3. Operation of the synchronous flyback converter

A SFB converter is operated as an isolated buck-boost converter. The building blocks of the SFB converter are simple to implement because it has a low component count. In general, SFB converters consist of two main switching devices, one capacitor and one transformer. Its topology is shown in Fig. 2.

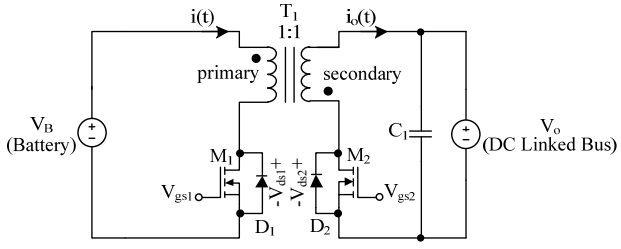

Fig. 2 The configuration of the bidirectional flyback converter

The SFB's operating principle (key waveforms shown in Fig. 3, operating modes shown in Fig. 4) can be described by eight basic stages as follows:

1. First stage (interval t_1): Switch M_1 is on. The energy from V_B will be stored in the flyback transformer (T_1). In this stage, current i(t) is rising and current $i_o(t)$ is equal to zero. The voltage drop across the drain and source pins of switch M_1 (V_{ds1}) is equal to zero. The voltage drop across drain and source pins of switch M_2 (V_{ds2}) is equal to the sum of V_B and V_o.

2. Second stage (interval t_2): While switch M_1 is off, the stored energy from T_1 begins to charge a parasitic capacitance of switch M_1. In the same time, switch M_2 is force-turned on to transfer energy from transformer T_1 to C_1 as a synchronous switch until energy from T_1 is zero.

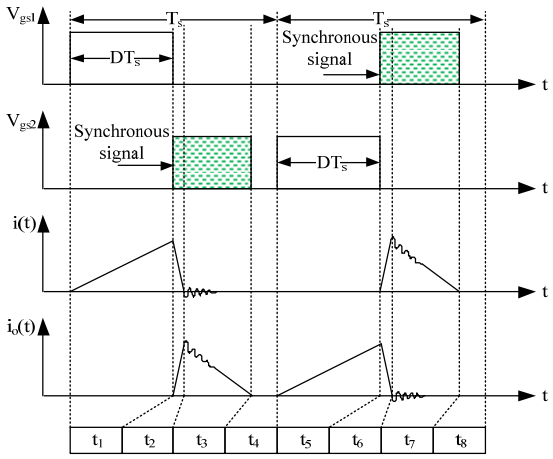

Fig. 3 Key waveforms of the proposed converter

3. Third stage (interval t_3): The current i(t) begins to decease as the energy stored in transformer T_1 drops. The voltage V_{ds1} is equal to the sum of V_B and V_o.

4. Fourth stage (interval t_4): In this stage, the currents i(t) and $i_o(t)$ are equal to zero. The voltage V_{ds1} is equal to the potential of V_B added to the resonant energy generated from the secondary winding of transformer T_1 and the parasitic capacitance of switch M_2. Switch M_2 is off.

5. Fifth stage (interval t_5): As switch M_2 is turned on, the energy from V_o will be stored in transformer T_1. In this stage, current $i_o(t)$ is rising and current i(t) is equal to zero. The voltage V_{ds2} is equal to zero. The voltage V_{ds1} is equal to the sum of V_B and V_o.

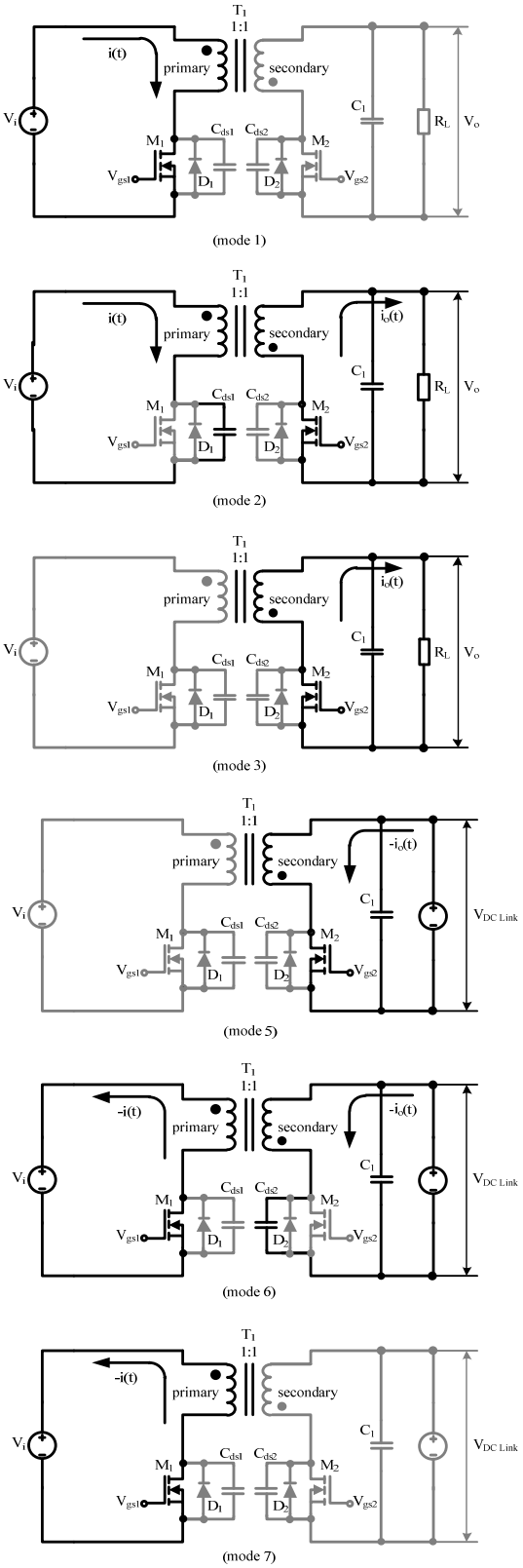

Fig. 4 Operating mode of the SFB converter Balanced Charging of Series Connected Battery Cells

6. Sixth stage (interval t_6): While switch M_2 is turned off, the stored energy from T_1 begins to charge the parasitic capacitance of switch M_2. In the same time, switch M_1 turned on for transfer energy from transformer T_1 to V_B as a synchronous switch until energy from T_1 is zero.

7. Seventh stage (interval t_7): The current $i_o(t)$ begins to decease as the energy stored in transformer T_1 drops. The voltage V_{ds2} is equal to the sum of V_B and V_o.

8. Eighth stage (interval t_8): In this stage, the currents $i_o(t)$ and i(t) are equal to zero. The voltage Vds2 is equal to the potential of V_o added to the resonant energy generated from the primary winding of transformer T_1 and the parasitic capacitance of switch M_1. The voltage V_{ds1} is equal to V_B added to the voltage across the primary winding of transformer T_1. Switch M_1 is turned off.

4. Design of the synchronous flyback converter

This section presents a guide to calculate the component of the SFB converter including the primary transformer inductance Lp, secondary transformer inductance Ls and the capacitor Co. The pre-defined input variable of the SFB converter is shown in Table 1.

Table 1 Pre-define input variable of SFB converter

Input Variable	Value
Maximum input voltage (V_{IN_max})	**7.5 V**
Minimum input voltage (V_{IN_min})	**6 V**
Nominal input voltage (V_{IN_norm})	**7 V**
DC-Linked bus voltage (V_{DC_LK})	**7.5 V**
Power output of each converter (P_O)	**8 W**
Switching frequency (f_{sw})	**20 kHz**
Switching period (T)	**$50x10^{-6}$ S**
Transformer efficiency (η_{Tr})	**0.9**
MOSFET turn on resistance (Rds_{on})	**0.024 Ω**

The maximum drain source voltage is computed by

$$Vds_{on} = \frac{Po}{\eta_{Tr} \times V_{IN\_min}} \times Rds_{on} = \frac{8}{0.9 \times 6} \times 0.024 = 0.0356\ V \quad (3)$$

If the nominal desired turn-on duty cycle (D_{norm}) is 0.5, the transformer turn ratio can be calculated by

$$N_{PS} = \left(\frac{V_{IN\_norm} - Vds_{on}}{V_{DC\_LK}}\right) \times \left(\frac{D_{norm}}{1 - D_{norm}}\right) = \left(\frac{7 - 0.0356}{7.5}\right) \times \left(\frac{0.5}{1 - 0.5}\right) = 0.9286 \cong 1 \quad (4)$$

The primary flyback mutual inductance voltage is also computed from

$$V_{fm} = N_{ps} \times (V_{DC\_LK} + Vds_{on}) = 1 \times (7.5 + 0.0356) = 7.536\ V \quad (5)$$

Maximum voltage across the main MOSFET (by using a safety factor at 115%) is estimated by

$$Vds_{max} = 1.15 \times (V_{IN\_max} + V_{fm}) = 1.15 \times (7.5 + 7.536) = 17.291\ V \quad (6)$$

The maximum turn-on time is calculated by

$$Ton_{max} = \frac{V_{fm} \times T}{(V_{IN\_min} - Vds_{on}) + V_{fm}} = \frac{7.536 \times 50 \times 10^{-6}}{(6 - 0.0356) + 7.536} = 27.91\ \mu S \quad (7)$$

The minimum turn-on time is calculated by

$$Ton_{min} = \frac{V_{fm} \times T}{(V_{IN\_max} - Vds_{on}) + V_{fm}} = \frac{7.536 \times 50 \times 10^{-6}}{(7.5 - 0.0356) + 7.536} = 25.12\ \mu S \quad (8)$$

The maximum duty cycle is calculated as

$$D\max = \frac{Ton_{max}}{T} = \frac{27.91 \times 10^{-6}}{50 \times 10^{-6}} = 0.558 \quad (9)$$

The minimum duty cycle is calculated as

$$D\min = \frac{Ton_{min}}{T} = \frac{25.12 \times 10^{-6}}{50 \times 10^{-6}} = 0.502 \quad (10)$$

The primary current ramp amplitude is calculated by

$$\Delta I_{pa} = \frac{2 \times P_o}{(V_{IN\_min} - Vds_{on}) \times \eta \times D_{max}} = \frac{2 \times 8}{(6 - 0.0356) \times 0.9 \times 0.558} = 5.342\ A \quad (11)$$

$$L_P = \frac{(V_{IN\_min} - V_{ds\_on})}{\Delta I_{pa}} \times Ton_{max} = \frac{(6 - 0.0356)}{5.342} \times 27.91 \times 10^{-6} = 31.162\ \mu H \quad (12)$$

$$L_s = L_p = 31.162\ \mu H \quad (13)$$

The secondary current amplitude is

$$\Delta I_s = \frac{(V_{DC\_LK} + Vds_{on}) \times (T - Ton_{max})}{L_s} = \frac{(7.5 + 0.0356) \times (50 \times 10^{-6} - 27.91 \times 10^{-6})}{31.162 \times 10^{-6}} = 5.3418\ A \quad (14)$$

The minimum output capacitance (maximum output ripple, V_{rp_max}) is

$$C_o = \Delta I_s \times \frac{Ton_{max}}{V_{rp_{max}} \times 0.25} = 5.342 \times \frac{27.91 \times 10^{-6}}{150 \times 10^{-3} \times 0.25} = 4{,}000\ \mu F \cong 4{,}700\ \mu F \quad (15)$$

From equations (3) to (15), the component variables of the SFB converter were calculated and their values are given in Table 2.

Table 2 The component variables of the SFB converter

Component	Value
MOSFET	IRFZ44E
Primary inductance (L_p)	31.162 μH
Secondary inductance (L_s)	31.162 μH
Transformer turn ratio	1:1
Output capacitor (C_o)	4,700 μF

5. Design of the fuzzy logic controller

The Main advantage of fuzzy logic control over other control methods is its simplicity and that a mathematical model is not required for the design of the system.

Moreover, it is compatible with nonlinear systems such as VRLA in a SCBS.

The fuzzy process was started at fuzzification by converting data input into a fuzzy set. Then, a fuzzy reasoning section computed the data. The result from this reasoning section was then sent to the defuzzification section. This was then used to control the real plant.

There were two input variables. The first variable was the current voltage (e). The other was the voltage error signal (e'). The output variable was a duty cycle command (U), which was sent to the CES for equalizing the unbalanced energy in the SCBS. The current voltage and voltage error signal were calculated from (16) and (17) respectively.

$$e = \text{input real voltage} \quad (16)$$

$$e' = \text{desired voltage-input real voltage} \quad (17)$$

The design of the fuzzy logic controller was accomplished by setting up the group of membership functions shown in Fig. 5. in the CEQ. The fuzzy inference was selected by Mamdani's method, and defuzzification was selected by the centroid method. Mamdani's inference algorithm and centroid defuzzification [18] are simple strategies for designing and implementing a control system by using a fuzzy set.

Table 3 The fuzzy logic rules used in CEQ

e/e'	NL	NM	ZE	PM	PL
NL	NL	NL	NL	NM	ZE
NM	NL	NL	NM	ZE	PM
ZE	NL	NM	ZE	PM	PL
PM	NM	ZE	PM	PL	PL
PL	ZE	PM	PL	PL	PL

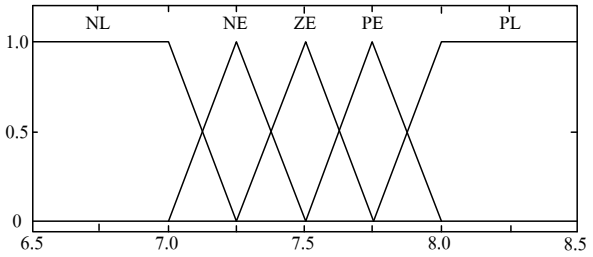

(a) The group membership functions of DC-Linked bus

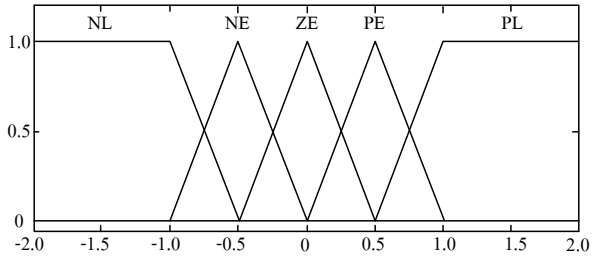

(b) The group membership functions of voltage error signal of DC-Linked bus

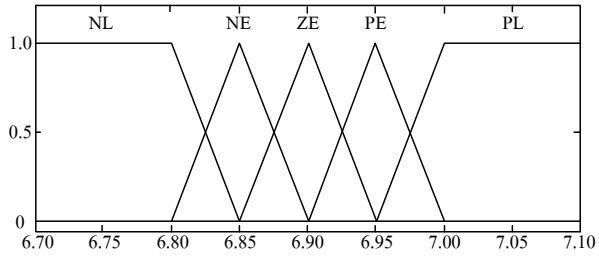

(c) The group membership functions of input battery voltage

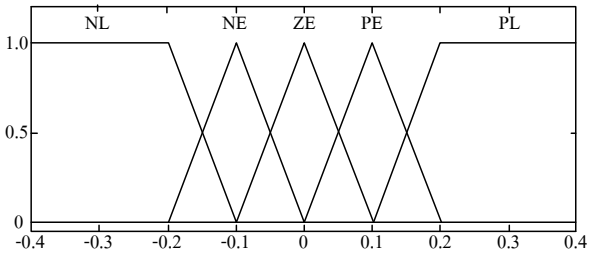

(d) The group membership functions of input error voltage of battery

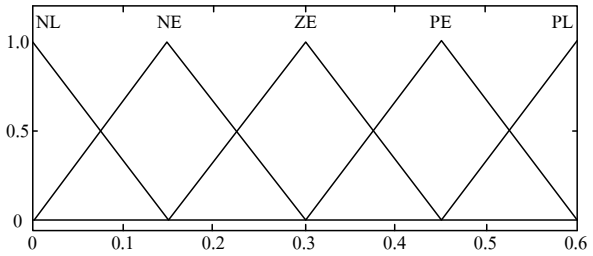

(e) The group membership functions of duty command signal

Fig. 5 The group membership functions of the fuzzy system using Mamdani and centroid technique

6. Simulation Results

To demonstrate the validity of operation of the fuzzy logic controller, it was simulated with a computer. The fuzzy logic rules are shown in Table 3. The initial system variables are shown in Table 4. The simulation consisted of two tested cases. First case, SCBS was charged without CEQ as shown in Fig. 6(a). Second case, SCBS was charged with CEQ under fuzzy-logic control, as shown in Fig. 6(b).

Table 4 Initial variables in the computer simulation of the fuzzy logic controller

Variable	Value
MOSFET (M_1, M_2)	IRFZ44N
Transformer (T_1)	L_p=L_s=32 µH
Capacitor (C_1)	4,700 μF
VRLA	12V/5AH, 4 units
Charging Current (I_s)	1,000 mA
Battery #1	SOC 95%
Battery #2	SOC 80%
Battery #3	SOC 90%
Battery #4	SOC 85%

The computer simulation showed that the fuzzy logic controller was able to control the power module of CEQ to equalize an energy imbalance of each of the batteries. At the beginning of the charging process, battery voltages increased rapidly and slowed down after one minute because of the internal chemical reactions of the VRLA battery. These battery voltages continued to increase for an additional 15 minutes. The voltage of battery number one reached voltage threshold. The fuzzy logic control system activated and generated a pulse width modulation (PWM) command to each CEQ's converter module. At the end of the charging process, the voltages of each battery were almost equal, and the fuzzy control system completely secured the VRLA in the SCBS by preventing it from an overcharging state. By integrating all membership functions along with the fuzzy logic rules. The fuzzy logic controller was now capable of controlling the power module

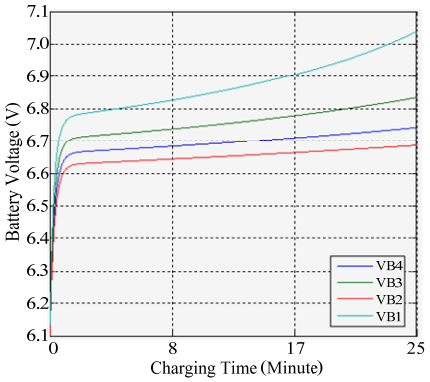

(a) Charging SCBS without CEQ

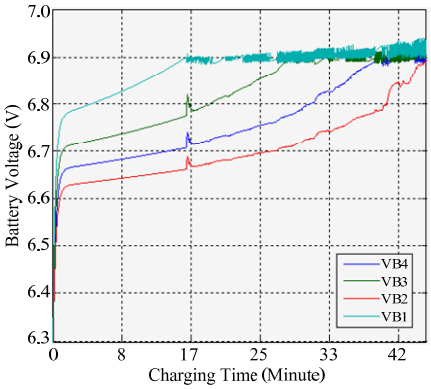

(b) Charging SCBS under fuzzy-controlled CEQ

Fig. 6 The simulation results of charging SCBS

7. Experimental Results

Four battery units with four different states of charge were used. Each battery was connected together in a serial configuration. A uniform power source fed the same charging current to these batteries. Two batteries, one charged by SFB-CEQ and another charged without CEQ were compared. Charging without CEQ caused some battery voltage to reach an overvoltage-floating charge level capable of damaging the battery.

In contrast, charging with CEQ controlled the battery charge with uniform voltages to all batteries. A PC computer

recorded the battery voltage data. The equipment used in this experiment was: a laboratory power supply (Model GPS-4303, GWINSTEK) provided the charge to SCBS; an oscilloscope (DS1022C, RIGOL) measured the converter's electrical signal waveforms; a true RMS digital multi-meter (FLUKE179, FLUKE) monitored the battery voltages; and battery SL6-5 (SPA® VRLA battery 6 V/5AH) was the test subject.

The operating frequency of the CEQ system was 20 kHz. The initial conditions of the four batteries at different state of charge (SOC) were: B1=6.02 V, B2=5.85 V, B3=5.92 V and B4=5.78 V.

To manage the unbalanced individual energies in the battery string, CESs were employed. Fig. 7 shows the battery voltages while charging with the CESs. The initial state of charging is depicted in the beginning region of Fig. 7, and it shows that each battery started at a different voltage. In the middle state of charging, 165 minutes later, the voltage of battery number 3 was 6.9 volt. At this point, the CESs started to control the unbalanced energy of each battery by passing the excess energy from the fully charged battery 3 to another battery unit at a lower voltage level. At the end of the charging process each battery had the same voltage.

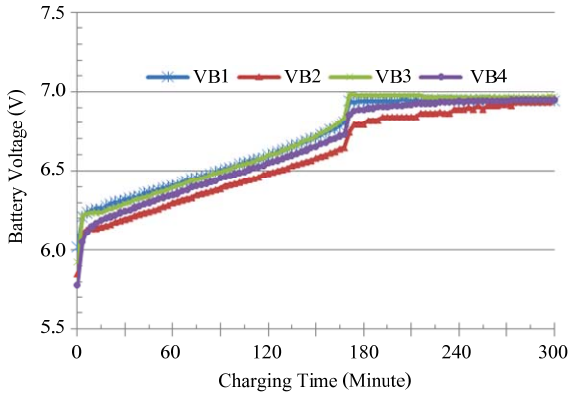

Fig. 7 The relationship of battery voltage and charging time

The oscillograms of a SFC are shown in Fig. 8. The relationship between the primary gate driving signal and a secondary synchronous-gate driving signal are shown in Fig. 8(a). A synchronous gate driving signal of the secondary switch (Fig. 8-a2) was instantly generated after the primary gate driving signal was turned off (Fig. 8-a1). The relationship between the drain-source voltages of the secondary switch (Fig. 8-b1) and the secondary synchronous-gate driving signal (Fig. 8-b2) are shown in detail. Both the voltage stress and the voltage spike of the secondary switch were low, suggesting that a low voltage component for this circuit could be used. In commercial terms, use of low voltage component is more economical and the reliability of a low stress system is higher.

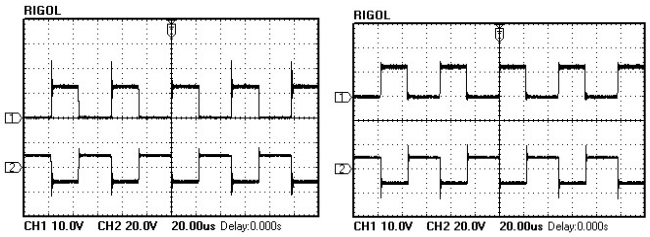

(a) (b)

Fig. 8 Detailed converter voltage waveforms (a-1) primary gate driving signal (a-2) versus secondary synchronous-gate driving signal, (b-1) drain-source voltage of secondary switch versus (b-2) secondary synchronous- gate driving signal

A comparison of the converter efficiency between the FB and SFB converters is shown in Fig. 9. The secondary switch of the SFB converter was turned on while the storage energy in the FB transformer transferred to load. The conduction loss of the SFB's secondary switch was low.

The maximum efficiency of the SFB converter was 78.9 percent at a power output of 6.7 watt. This efficiency of the SFB converter was better by up to 1.07 percent over the conventional FB converter, which was 77.2 percent at the same power level.

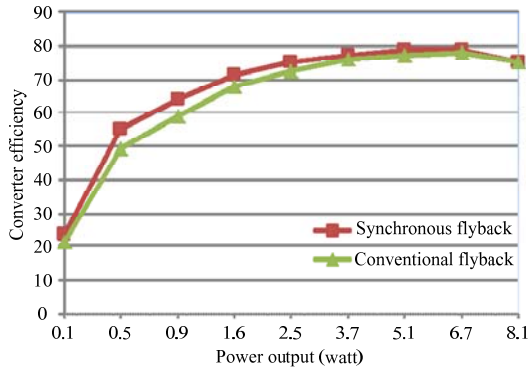

Fig. 9 The efficiency comparison between the conventional FB converter and the SFB converter

The small difference of the efficiency of the converter at a rated power of 3.7 w to 8.1 w could come from the secondary synchronous gate-driving signal that consumed energy directly from the SFB's transformer. In this high power region, duty cycles of the PWM signal were greater than previously rated and took more energy than in a low power region.

8. Conclusion

The tested SFB converter satisfactorily improved total converter efficiency. It was practical to implement a high efficiency battery management system by incorporating a SFB converter and a fuzzy logic controller into the battery equalization process. This converter-controller combination eliminated the problem of unbalanced battery voltages. The experimental results showed that the conduction loss at the secondary switch in the SFB was minimized and as a result, the total converter efficiency increased to 78.9 percent at a power output of 6.7 watt. The proposed SFB converter-controller has a modularized design and is simple to construct, install and maintain. In future work a SFB converter with high power output and one-cycle control will be studied, because the advantages are fast control and applicability to linear and nonlinear systems.

9. Acknowledgements

We thank Dr. Rainer Zawadzki for editing the manuscript. We also would like to thank the Rajamangala University of Technology Lanna as part of a project entitled "Hand-on research and development".

10. References

[1] http://www.panasonic.com/industrial/batteries-oem/oem/lead-acid-vrla.aspx, February 2011.

[2] http://www.bb-battery.com/techmanual.asp, February 2010.

[3] S. Bergvik, "Prolonged Useful Life and Reduced Maintenance of Lead - acid Batteries by Mean of individual Cell Voltage Regulation" INTELEC Conference, 1984, pp. 63 - 66.

[4] D. Bjork, "Maintenance of Batteries-new trend in batteries and automatic battery charging", IEEE INTELEC Conference, 1986, pp. 355-360.

[5] D. C. Hopkins, "Dynamic Equalization During Charging of Serial Energy Storage Element", IEEE IEEE Transactions on Industry Applications, 29, 1993, pp. 363-368.

[6] N. H. Kutkut and Divan, D. M., "Dynamic Equalization Technique for Series Battery Stacks", IEEE INTELEC, 1996, pp. 514-521.

[7] C. Pascual and P. T. Krein, "Switched Capacitor System for Automatic Series Battery Equalisation", IEEE APEC Conference, 2, 1997, pp. 848-854.

[8] H. Sakamoto, K. Murata, E. Sakai, K. Nishijima, K. Harada, S. Taniguchi, K. Yamasaki and G. Ariyoshi, "Balanced Charging of Series Connected Battery Cells", IEEE Telcom. Energy Conference, 1998, pp. 311-315.

[9] N. H. Kutkut, H. L. N. Wiegman, D. M. Divan and D. W. Novotny, "Design Considerations for Charge Equalization of an Electric Vehicle Battery System",

IEEE Transactions on Industry Applications, 35, 1999, pp. 28-35.

[10] S. West and P. T. Karin, “Equalization of Valve Regulated Lead-Acid Batteries: Issues and Life Test Results”, IEEE Telc. Energy Conf., 2000, pp. 439-446.

[11] Y. C. Hsieh, C. S. Moo and I. S. Tsai, “Balance Charging Circuit For Charge Equalization”, IEEE Conf. PCC Osaka, 2002, pp. 1338-1141.

[12] C. Karnjanapiboon, Y. Rungruengphalanggul and I. Boonyaroonate, “The Low Stress Voltage Balance Charging Circuit for Series Connected Batteries Based on BUCK-BOOST Topology”, IEEE ISCAS Conf., 3, 2003, pp. 284-287.

[13] A. C. Baughman and M. Ferdowsi, “Double-tiered switched-capacitor battery charge equalization technique”, IEEE Trans. Ind., 55, 2008, pp. 2277-2285.

[14] P. Hong-Sun, K. Chong-Eun, K. Chol-Ho, M. Gun-Woo and L. Joong-Hui, “‘A Modularized Charge Equalizer for an HEV Lithium-Ion Battery String”, IEEE Trans. Ind. Elec., 2009, pp. 1464-1476.

[15] Y. S. Lee and M. W. Cheng, “Intelligent Control Battery Equalization for Series Connected Lithium-Ion Battery Strings”, IEEE Trans. Ind., 52, 2005, pp. 1297-1307.

[16] C. Karnjanapiboon, K. Jirasereeamornkul and V. Monyakul, “High efficiency battery management system for serially connected battery string”, IEEE ISIE Conf., 2009, pp. 1504-1509.

[17] Y. Jingyu, C. Zhu, X. Guoqing, Q. Huihuan and X. Yangsheng, "Fuzzy Control for Battery Equalization Based on State of Charge," Vehicular Technology Conference Fall (VTC 2010-Fall), 2010, pp. 1-7.

[18] S. N. Sivanandam, S. Sumathi and S. N. Deepa, “Introduction to fuzzy logic using MATLAB”, Springer, 2007.